*Institute of Space and Aeronautical Science, University of Tokyo*
*Report No. 491, May 1973*

# Reception Characteristics of Monopole Antennas for Electron Plasma Waves

*By*

Yoshiharu NAKAMURA, Masaharu NAKAMURA and Tomizo ITOH

*Summary* : The radiation patterns of a longitudinal electron wave excited in a warm plasma by parallel plane grids and the reception patterns of wire antenna were measured experimentally, and the results agreed with the theoretically predicted radiation pattern. The reception patterns of a gridded parallel plate antenna are sharper than the theoretical radiation pattern and the sharpness depended on width of its guard ring. The dependence of the received amplitude on the D. C. potential of the antennas was studied. The possibility of estimating the wavelength from measured amplitudes is also discussed.

## 1. INTRODUCTION

To date, several kinds of monopole antennas, for example, a wire probe [*1*], a gridded parallel plate coupler [*2*] and parallel plate grids [*3, 4*] have been used to excite and to detect the electron plasma wave in the laboratory experiments. However, these experiments did not include any measurement of antenna characteristics i.e. radiation and reception patterns and detection efficiency. Recently, radiation patterns for some simple antennas to transmit ion-acoustic wave have been measured by K. Shen et al. [*5*]. Their results tended to agree with the theoretically predicted radiation pattern based on the plasma fluid model. With reference to electron plasma wave, the radiation patterns for grid antenna were measured experimentally by T. Ishizone et al. [*6*] The receiving patterns and reception characteristics of the antennas were not clear in their experiments.

In space experiments, a dipole and a loop antenna on a spacecraft were used to observe spontaneous electrostatic wave by F. L. Scarf et al. [*7*] In this study, frequency and intensity of waves were measured. Dipole antenna loses its directionality if antenna dimension is smaller than the wavelength of received plasma wave. [*5*] To know the direction of wavenumber vector of the wave, it is desirable to use the detector having a sharp reception pattern. Furthermore, it is necessary to measure the wavelength of static wave caused by some instabilities.

It is the purpose of this work to examine experimentally the detection characteristics of some monopole antennas for electron plasma waves and to compare them with a simple theoretical model.

In § 2 the theoretical radiation patterns based on an electron fluid model are introduced. Experimental procedure is described in § 3. We give experimental results in § 4 and discuss them in § 5.

## 2. Theoretical Radiation Patterns

In order to estimate the radiation pattern of longitudinal electron wave in an unbounded plasma, it is simple to use electron fluid model. The equation of motion for electrons is written as

$$\frac{\partial \boldsymbol{V}}{\partial t}=\frac{e}{m}\boldsymbol{E}-\frac{\gamma\kappa T_e}{mn_0}\nabla n_1, \tag{1}$$

where $\boldsymbol{V}$ is the electron velocity, $e$ is the charge of electrons, $m$ is the electron mass, $\gamma$ is the ratio of specific heats, $T_e$ is the electron temperature, $\kappa$ is Boltzmann's constant, $\boldsymbol{E}$ is the perturbed electric field and $n_0$ and $n_1$ are the unperturbed and perturbed electron density, respectively. Here collision term is neglected, since in experimental condition mean free path of electron-neutral atom collisions is larger than the chamber dimensions. The equation of continuity for electrons is

$$\frac{\partial n_1}{\partial t}+n_0 \operatorname{div} \boldsymbol{V}=0. \tag{2}$$

Poisson's equation is

$$\operatorname{div} \boldsymbol{E}=4\pi e n_1+4\pi\rho_{ex}, \tag{3}$$

where we have included $\rho_{ex}$ as an external source term. Solving (1) through (3), we obtain an equation for $n_1$,

$$\Delta n_1-\frac{1}{\gamma V_{\mathrm{th}}^2}\frac{\partial^2 n_1}{\partial t^2}-\frac{\omega_p^2}{\gamma V_{\mathrm{th}}^2}n_1=\frac{4\pi e n_0}{\gamma\kappa T_e}\rho_{ex}$$

where

$$\omega_p^2=\frac{4\pi e^2 n_0}{m} \quad \text{and} \quad V_{\mathrm{th}}^2=\frac{\kappa T_e}{m}.$$

Since the phase velocity of electron plasma wave is much smaller than the light velocity, time-varying magnetic field can be neglected. For a time dependence $\exp(i\omega t)$, we obtain a wave equation

$$\Delta n_1+K^2 n_1=\frac{4\pi e n_0}{\gamma\kappa T_e}\rho_{ex}, \tag{4}$$

where

$$K^2=\frac{\omega^2-\omega_p^2}{\gamma V_{\mathrm{th}}^2}. \tag{5}$$

Equation (4) is an inhomogeneous Helmholtz equation. Its solution is written as

$$n_1(\boldsymbol{r})=\frac{e n_0}{\gamma\kappa T_e}\int_{V'}\frac{\rho_{ex}(\boldsymbol{r}')\exp\left[-iK|\boldsymbol{r}-\boldsymbol{r}'|\right]}{|\boldsymbol{r}-\boldsymbol{r}'|}dV' \tag{6}$$

where the primed coordinate refers to the source.

As the antenna dimensions are much less than the free-space wavelength, it is reasonably assumed that a charge distribution is uniform on an antenna surface. It is also assumed that the position considered is far from the antenna, i.e. $r \gg L$, where $L$ is the dimension of antenna. After the Eq. (6), the radiation pattern for the wire antennas $B$ and $C$ of length $L$ in Fig. 2 can be expressed as

$$n_1(r, \theta) = \frac{Len_0\rho}{\gamma\kappa T_e}\left[\frac{\sin(\frac{1}{2}KL\sin\theta)}{KL\sin\theta}\right]\frac{e^{-ikr}}{r} \qquad (7)$$

and for a circular disc antenna of diameter $L$,

$$n_1(r, \theta) = \frac{\pi L^2 en_0\rho}{\gamma\kappa T_e}\left[\frac{J_1(\frac{1}{2}KL\sin\theta)}{KL\sin\theta}\right]\frac{e^{-ikr}}{r} \qquad (8)$$

in spherical coordinate where the polar axis is defined as the line peperpendicular to the center of the disc or the wire, $\rho$ is the charge per unit area or unit length, and $J_1$ is the Bessel function of order 1. The terms in the brackets in Eq. 7 and Eq. 8 will be used to predict the radiation or receiving patterns of electron plasma waves for monopole antennas. In deriving the wave equation from the fluid theory, we could neglect the collision damping taking experimental condition into consideration. However, even in the absence of collisions, waves are attenuated by Landau damping which is deduced from the theory based on kinetic equations. Correction of Eqs. (7) and (8) due to wave damping is maximum at $\theta = 90°$ and it is order of $(K_i/K_r)^2$ if $K_i/K_r \ll 1$, where $K_r$ and $K_i$ are real and imaginary part of $K$. In our experiment, the ratio $K_i/K_r$ was at most about 0.2 so that correction due to damping can be neglected.

## 3. Experimental Procedure

The experiment was performed using the space chamber shown shematically in Fig. 1. At both ends of the chamber plasma sources of glow-mode type which has an oxide cathode and a mesh anode 150 mm in diameter are set up face to face [*8*]. The stainless steel chamber and the anodes were grounded. The measurement was done under continuous pumping and bleeding of Argon gas into the chamber through a needle valve. The base pressure in the chamber was kept beneath $5\times10^{-7}$ Torr and a working gas pressure was $1\sim3\times10^{-4}$ Torr. The discharge voltages between the anodes and the cathodes were 40~60 V. The plasma was created by ionizing collisions of primary electrons accerelated by the screen anode with the background Argon atoms. Density of the plasma in the region of measurement was homogeneous and it was about $2\times10^6/\text{cm}^3$. Electron temperature measured with a Langmuir probe depended on gas pressure and was about 4 eV. A transmitting disk grids whose diameter L is 18 cm consisted of three tungsten meshes made of 0.03 mm diameter wires spaced 0.5 mm apart. Separation of each meshes was 5 mm.

As receivers three kinds of monopole antennas shown in Fig. 2 were used. Four gridded parallel plate couplers which are called Faraday cup type detectors in this

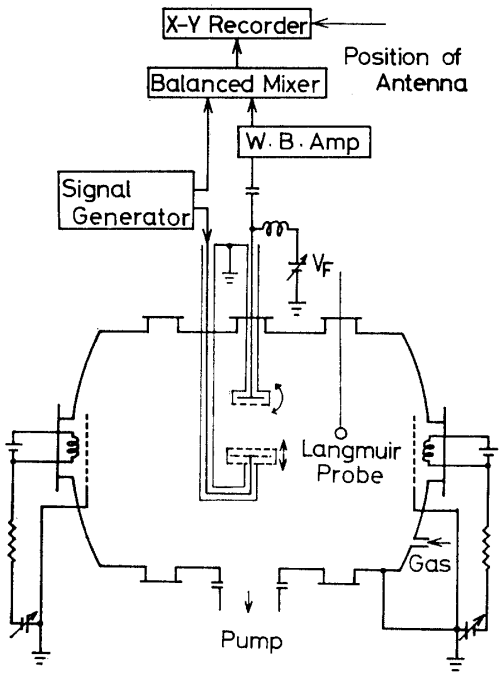


FIG. 1. Schematic diagram of the experimental apparatus.

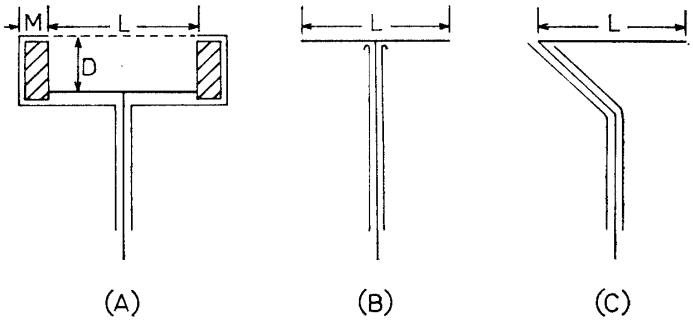


FIG. 2. Receiving antennas. (A) Faraday cup type antenna. (B) T-type wire probe antenna. (C) L-type wire probe antenna.

paper, designated as (a)~(d) in Fig. 2 (A), consisted of a molybdenum mesh made of 0.1 mm diameter wires spaced 1.2 mm apart and a collector. Their dimensions were (a) $L=100$, $D=20$, $M=25$ (b) $L=80$, $D=6$, $M=10$ (c) $L=80$, $D=20$, $M=10$ (d) $L=80$, $D=40$, $M=10$ in mm units. The outer grids of the transmitter and the receiver were grounded to reduce the direct coupling [2]. Antennas (B) and (C) in Fig. 2 were made of wire 1 mm in diameter whose length $L$ was equal to 100 mm. However, the position of the connecting coaxial cables was different as shown in Fig. 2. With antenna (B), which is called hereafter T-type, the cable was connected to the center of the wire, whereas with antenna (C), which is called L-type, the cable was connected to the end of the wire.

When the reception patterns for an antenna were measured, it was set at the center of the chamber and was rotated through 180°. The exciter was moved from

20 to 100 cm from the receiver as shown in Fig. 1. When radiation patterns for the transmitter were observed, it was rotated and the receiving antenna was moved. A signal picked up by the antennas was fed into a bias insertion unit, a wide-band amplifier and a balanced mixer. A reference signal from the signal generator was added to the mixer; i.e., the system was used as an interferometer. The position of the transmitter grids or receiver was taken as the $x$ axis of an $x$–$y$ recorder, and the mixer output applied to the $y$ axis.

## 4. Experimental Results

(A) Radiation patterns of the monopole mesh antenna.

We first experimentally measured the dispersion relation [*4*]. The observed dispersion diagram is shown in Fig. 3. Ordinate is wave frequency normalized by $\omega_p$ and abscissa is wavenumber normalized by Debye wavenumber $K_D=\omega_p/V_{\text{th}}$. Crossed points and closed circles are measured imaginary and real part of the normalized wavenumber, respectively. Density and temperature of electrons were determined by Langmuir probe characteristics. Theoretically we can not compare it with the dispersion relation Eq. (5) which is based on fluid model but with the following relation obtained from kinetic equations

$$\frac{K_D^2}{2K^2}Z'(\omega/\sqrt{2}KV_{\text{th}})=1 \qquad (9)$$

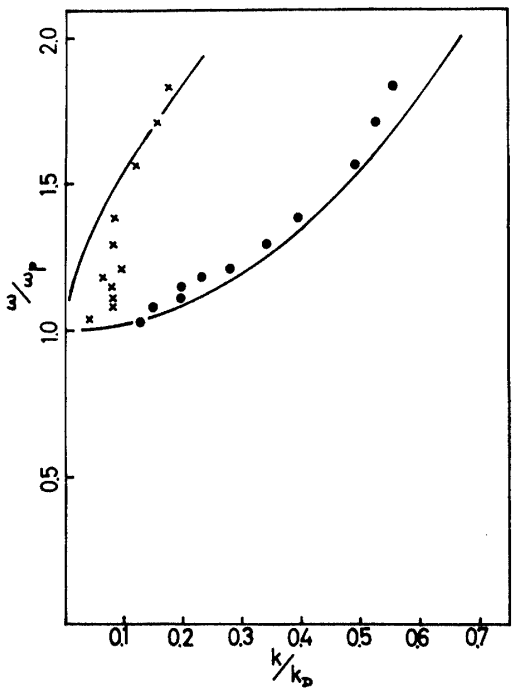


FIG. 3. Dispersion relation. Closed circles and crossed points are experimental real and imaginary part of the normalized wave number, respectively. Solid lines are theoretical curves given by Eq. (9).

where $Z'$ is the derivative of the plasma dispersion function [9]. Solid curves are theoretical real and imaginary part of wavenumber given by Eq. (9). The figure shows the investigating wave is not electron free-streaming observed in the lower frequency than about $\omega_p$ but the electron plasma wave [10].

We next obtained wave propagation patterns for the disk grids as a function of angle by the interference method stated in the previous section. Angle $\theta$ is zero when the plane of grids faces to the receiving antenna. Typical raw propagation patterns as drawn by the $x$–$y$ recorder are shown in Fig. 4. D. C. potential of central grid of exciter was zero, about 2 V lower than plasma potential and high frequency voltage applied to the grid from the signal generator was 6V peak to peak. A radiation pattern for the transmitter is shown in Fig. 5 (b) by plotting the amplitude at the fixed distance from the transmitter. The solid curve is a theoretical line predicted from Eq. 8. Plots of position of crest (crossed points) and trough (closed circles) in $x$–$y$ raw data like Fig. 4 is shown in Fig. 5 (a). It clearly shows that a spherical wave propagates from the antenna. It also shows that at angle larger than about 45°, the position of crest and trough is reversed, that is, phases differ from each othe rby 180° at constant distance from the center of the

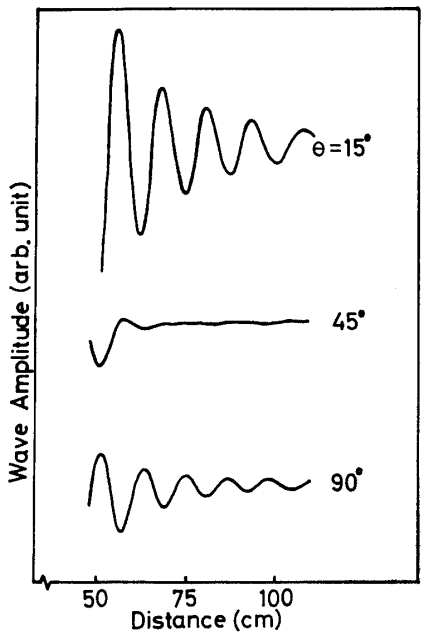


FIG. 4. Raw data. $\omega/2\pi=19.0$ MHz.

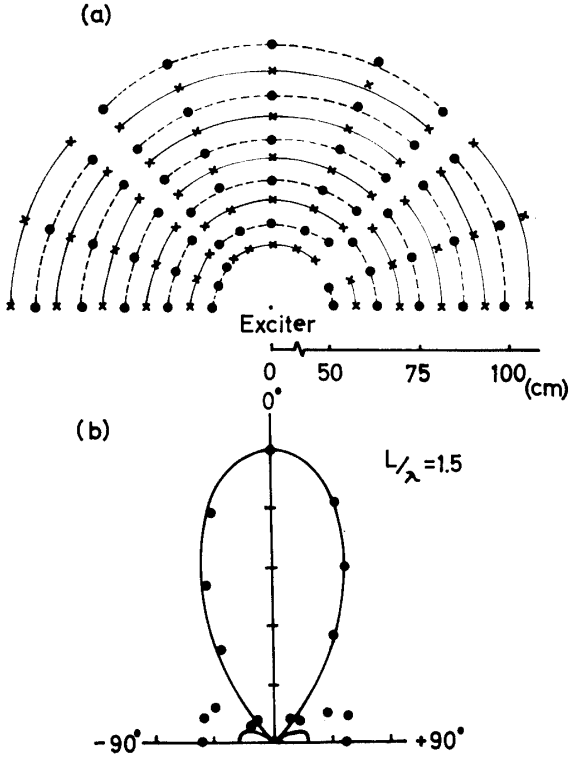


FIG. 5. (a) Position of crest and through in raw data shown in Fig. 4.
(b) Closed circles: Experimentally measured radiation pattern. $\omega/2\pi=$ 19 MHz. Experimental $L/\lambda=1.4$. Solid line: Theoretical curve given by Eq. (8) using $L/\lambda$ as 1.5.

exciter. This is explained theoretically by considering Eq. 8. When $L/\lambda=1.5$ ($\lambda$: wavelength) the numerator of Eq. 8 is zero at $\theta=45°$ and it becomes negative at larger $\theta$ due to the sign of the Bessel function.

Typical radiation patterns are shown in Fig. 6 along with the patterns predicted from Eq. 8. Here, a wire probe of 1 mm in diameter and 50 mm in length was used as a receiving antenna. Distance at which the amplitude is read is farther than 50 cm from the transmitter. The parameter of $L/\lambda$ written in the figure is the theoretical variable which is fit to the experimental results. In general, the experimental $L/\lambda$ values are about ten percent smaller than shown in Fig. 6. It was, therefore, considered that they agree well with the predicted radiation patterns in experimental errors due to finite size of the receiver and limitations imposed by our use of the far-field approximation and by neglect of damping of wave in the calculation.

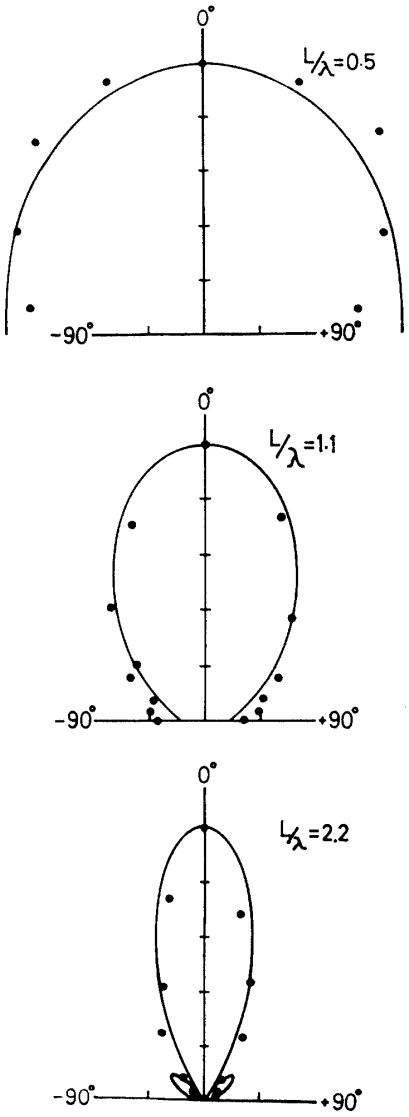


FIG. 6. Theoretically predicted and experimentally measured radiation patterns for parallel mesh grids.

(B) Receiving characteristics of Faraday cup type detectors

The receiving patterns for the Faraday cup type antennas were obtained by measuring the amplitude of the received electron plasma wave signal as the receiving antenna was rotated as shown in Fig. 1. As distance between the exciter and the receiver was about 50 cm so that wave was considered as plane wave for detectors of 10 cm in diameter. Then receiving patterns for an antenna was equal to radiation patterns for it taking reciprocity theorem into consideration. As the structure of Faraday cup type antenna was similar to the three mesh exciting grids, its reception patterns seemed to be the same as radiation patterns of the disk grids. D. C. potentials of the mesh and the collector of the cup were zero and floating, respectively. Some typical receiving patterns of the cup (a) are shown in Fig. 7. Small closed circles are the experimental values and dotted lines are radiation patterns predicted from Eq. 8 using experimental $L/\lambda$ values. Measured values disagree with theoretical ones. The receiving patterns are sharper than the predicted and they coincide with the theoretical patterns of $L/\lambda \approx 2$ which can not be obtained experimentally when instead of 100 mm, diameter 150 mm ($L + 2M$ in Fig. 2) is used as $L$. This discrepancy is due to the structure of the detectors, that is, finite depth $D$ and guardring width $M$ which are not taken into account in the theory. We tested another three Faraday cup type detectors named (b)~(d) introduced in the previous section which had the same $L$ and $M$ dimensions but had different depth $D$. Receiving patterns of the detectors for the same experimental $L/\lambda$ values are shown in Fig. 8. They have similar patterns each coinciding with the radiation pattern of $L/\lambda = 1.0$ given by Eq. 8. Disagreement between the measurement points and the dashed line in the Fig. 8 decreased when the receiving pattern was established at $L/\lambda > 1.0$. In these cases, the difference between the experimental $L/\lambda$ and the theoretical $L/\lambda$ fitting the measured pattern is not so large in comparison with the case of Faraday cup type detector (a). For Faraday cup type detector (a), the ratio $M/L = 0.25$ and for detectors (b)~(d) the ratio $M/L = 0.13$. From the experimental results stated above, we consider that discrepancy between the measured and predicted patterns for small $L/\lambda$ value is due to the effect of the guard ring. However, the received intensity of them was not the same, it is inversely proportional to depth $D$ within experimental errors. This is explained as follows. The collector shown Fig. 2 (A) picks up the oscillating potential through a capacitive coupling between the plasma and the collector. The reactance $1/\omega C$ is much larger than the input impedance of the wide-band amplifier so that the amplitude of the detected signal is proportional to capacitance $C$ and is inversely proportional to depht $D$. At the floating otential, the *rf* conduction current flowing to the collector is negligible as described below.

Electron plasma wave is the oscillation of electron density as shown in sectron 2. Then, it is possible to detect the wave by collecting the fluctuating electrons. By varying the bias potential of the collector against a plasma potential, electron current imping on the collector changed like the curve (c) in Fig. 9. The received *rf* amplitude is also shown by the curve (b). Because below $-60$V electron current is considered as almost zero, wave is detected by its potential $\phi$ through the capa-

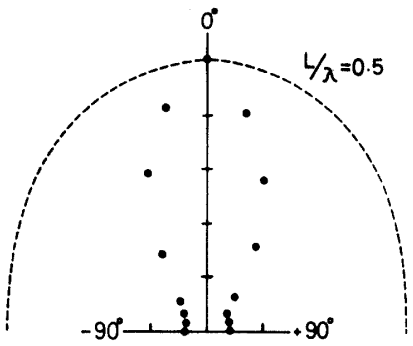


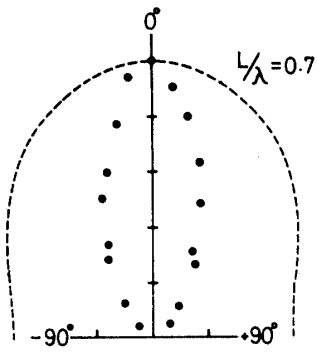


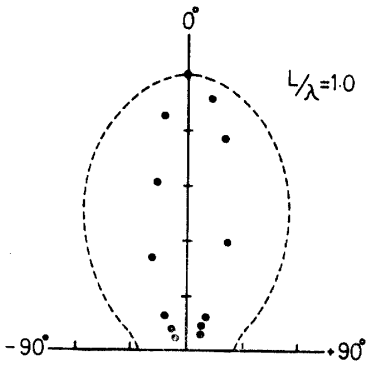


FIG. 7. Experimentally measured receiving patterns for the Faraday cup type detector (a). Dotted lines are theoretical radiation patterns given by Eq. (8) using experimental $L/\lambda$ values shown in the figure.

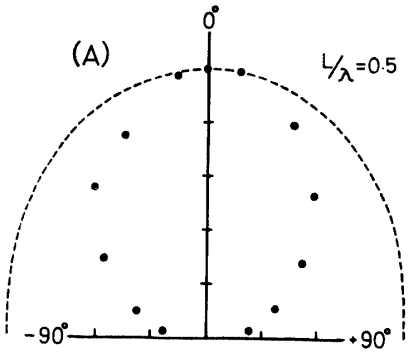


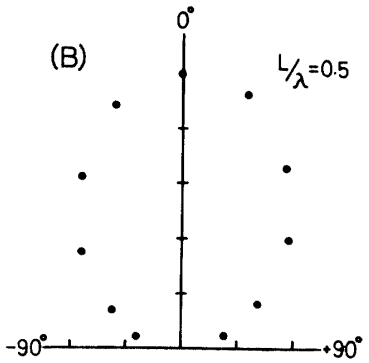


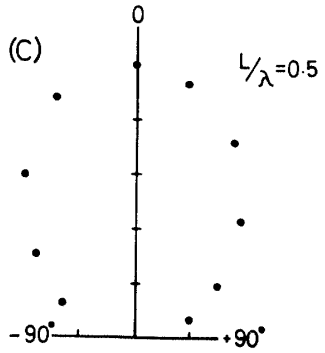


FIG. 8. Experimentally measured receiving patterns for the Faraday cup type detectors having different depth $D$. Dotted line is theoretical radiation pattern given by Eq. (8) using experimental $L/\lambda$ value.
(A) Detector (b). $D=6$ mm
(B) Detector (c). $D=20$ mm
(C) Detector (d). $D=40$ mm

citance between the collector and the plasma in flont of the mesh grid. Increasing the bias potential, electron current increases and shows behavior of saturation like Langmuir probe characteristics. Received amplitude is the sum of *rf* potentials due to the displacement and the conduction currents flowing into the electrode. The displacement current is proportional to the wave amplitude $\phi$, here $\phi$ is given by

$$\phi=\frac{4\pi en_1}{K^2} \tag{10}$$

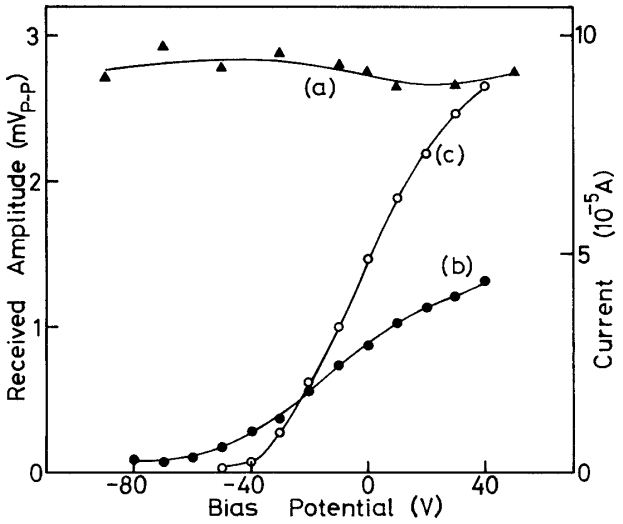


FIG. 9. Dependence of received amplitude on D.C. bias potential.
$\omega/2\pi=16.0$ MHz, $\lambda=13$ cm.
(a) Antenna (B) in Fig. 2. (b) Faraday cup detector (c).
(c) Electron current characteristic of the detector (c).

which is obtained from the equation $E=-\nabla\phi$ and the assumption that the considering point is far from the transmitter. The conduction current is proportional to the flux due to a part of electrons impinging to the electrode. As a result of it, if the displacement current is negligible, dependence of the received amplitude on the bias potential resembles that of the D. C. electron current. Experimentally the phase of the signal due to capacitive coupling and the phase of the amplitude due to impinging electrons seemed to be equal with each other at the same distance from the transmitter.

(C) Receiving characteristics of wire antennas

Directional patterns of the T-type antenna for some wavenumbers are shown in Fig. 10. Here, the disk grids were used again as the transmitter. Closed circles are the measured amplitude as a function of rotation angle of the antenna and the solid curves show radiation patterns estimated from Eq. (7). Parameters $L/\lambda$ written in the figure are theoretical variables which fit the experimental points. Experimenntal $L/\lambda$ values are larger than those of theory by at most 15 percent including experimental errors. In this case, contrary to the case of Faraday cup type detectors, the reception patterns agree with the calculated radiation patterns. The received amplitude vs D. C. bias voltage is shown in Fig. 9 as the curve (a). Current impinging to the antenna showed Langmur characteristics like curve (c) in Fig. 9. As seen from the figure the detection efficiency of this antenna is almost independent of the D. C. bias potential. The detection patterns of the antenna (C) in Fig. 2 are similar to those of antenna (B) shown in Fig. 10.

## 5. DISCUSSION

It is pointed out that a 50 $\Omega$ coaxial probe is sensitive to electric field so that the

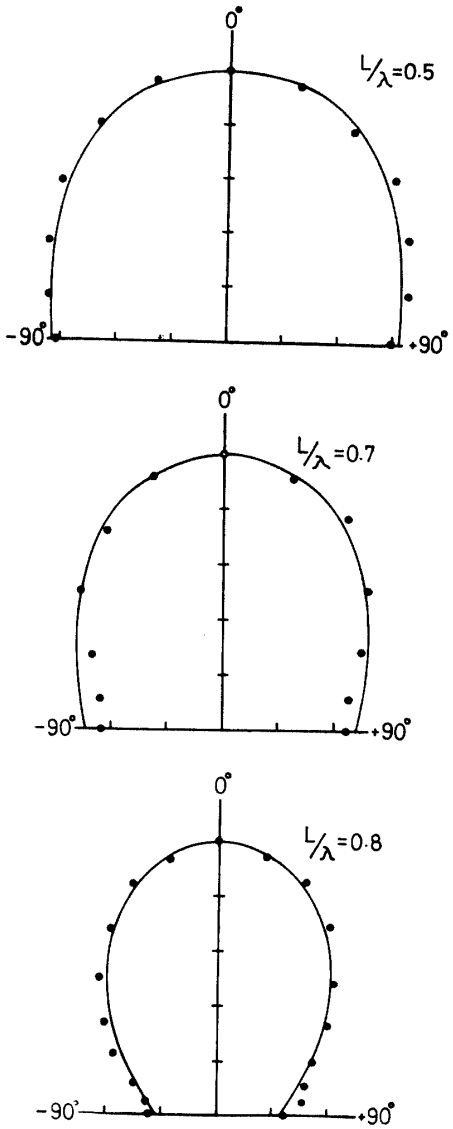


FIG. 10. Experimentally measured receiving patterns of the antenna (B) shown in Fig. 2. Solid lines are theoretically predicted (Eq. 7) radiation patterns.

observed voltage V is the line integral of the field along a path defined by the probe [*11*].

$$V = \int_{\text{prove}} \boldsymbol{E}(\boldsymbol{r}) \cdot d\boldsymbol{S} \tag{11}$$

Electron plasma wave is a longitudinal wave, i.e. the direction of electric field is parallel to the wave number vector. As a result of it, if the antenna picks up the electric field, the maximum received amplitude is obtained when the probe wire is parallel to the direction of the wave ($\theta = \pm 90°$) and the phase at $\theta = 90°$ must be different by 180° from the phase at $\theta = -90°$. Experimentally, however, the reception patterns of the L-type antenna were equal to those of T-type antenna. Received amplitudes at $\theta = 0°$ of both antenna were also nearly equal with each other. These

results suggest that these T-type and L-type antennas are sensitive to space charges of electron plasma wave through capacitive coupling and that the induced voltage by action described by Eq. (11) is negligible at least in the present case in which the input impedance of the antenna is small (50 $\Omega$).

Receiving antennas pick up wave potential $\phi$ by the displacement current and the conduction current. Received amplitude $\phi_R$ when the bias potential of the antenna is the plasma potential is the sum of *rf* potentials which are written as

$$\phi_D = \omega C R_0 \phi \tag{12}$$

and

$$\phi_C = en_1\left(\frac{\omega}{K}\right)SR_0 \tag{13}$$

where $C$ the effective capacitance between the antenna and plasma, $R_0$ is the input impedance and $S$ is surface area of the antenna. Here assumption $R_0 \ll 1/\omega C$ based on the experimental condition is used. Recently, electron density irregularities due to some instabilities in the equatorial ionosphere were observed by measurement of the *rf* conduction current and the electron D. C. current flowing to a Langmuir probe[12]. In this measurement, the displacement current might be neglected owing to its low frequency. For the wire antenna, $\phi_C$ is neglected compared with $\phi_D$ because of its small $S$. On the other hand, for the Faraday cup detector whose grounded mesh shields displacement current, $\phi_D$ is neglected compared with $\phi_C$ as shown in the previous section. In Fig. 9(a), $\phi_D$ of the T-type antenna is about 2.8 mV. We estimate $C$ as 0.96 *PF* from the relation $C = 2\pi\varepsilon_0 L/\log(D/a)$ assuming that equivalent sheath thickness $D$ is 5 cm which is about five times the Debye length $\lambda_D$ and $a = 0.5$ mm. At the floating potential sheath thickness is about five times $\lambda_D$. [*13*] In the present case, notwithstanding the antenna being at the plasma potential, $D$ is assumed to be five times $\lambda_D$. The reason is that at this potential the antenna absorbs electrons and its density around it is made sparse which is equivalently same to the ion-sheath. In reality $C$ depends weakly on $D$ due to its logarithmic dependence. Then $\phi$ equals about 0.58 $V_{p-p}$ after substituting $C$ and $\omega/2\pi = 16$ MHz into Eq. (12). Under the same wave propagation the received amplitude $\phi_C$ to the Faraday cup type detector is 1.1 mV at the plasma potential shown in Fig. 9. From Eq. (13), using $\phi_C = 1.1$ mV the perturbed density $n_1$ is estimated to be $8.4 \times 10^4/\text{cm}^3$. Here, equivalent area $S$ is one tenth of $\pi L^2/4$ due to the structure of the detector. This value was estimated from comparing the unperturbed saturation current of the detector with that of the Langmuir probe. Furthermore, using this value of $n_1$ and the experimental wavelength 13 cm, the wave potential $\phi$ is calculated to be 0.65 $V_{p-p}$ from Eq. (10). As a result, two independently obtained wave amplitudes agree with each other. This conclusion suggests that if we use both of these antennas we can compute the wavelength of the static wave from both received amplitudes.

## ACKNOWLEDGMENTS

The authors wish to acknowledge Professor S. Adachi of Tohoku University for discussions. They also thank Mr. S. Kojima, Mr. H. Koike and Mr N. Morita for their help with experiments.

*Division of Space Science,*
*Institute of Space and Aeronautical Science,*
*University of Tokyo, Komaba, Meguro-ku,*
*Tokyo, Japan*
*April 10, 1973*

## REFERENCES

[1] J. H. Malmberg and C. B. Wharton: Dispersion of electron plasma waves, Phys. Rev. Letters **17**, 175 (1966).
[2] Gerard Van Hoven: Observation of plasma oscillations, Phys. Rev. Letters **17**, 169 (1966).
[3] H. Derfler and T. C. Simonen: Landau waves: An experimental fact, Phys. Rev. Letters **17**, 171 (1966).
[4] T. Kawabe, Y. Kawai, O. Saka, Y. Nakamura and J. M. Dawson: Effects of electron-neutral collisions on propagation of electron plasma waves, Phys. Rev. Letters **28**, 889 (1972).
[5] K. Shen, S. Aksornkitti, H. C. S. Hsuan and K. E. Lonngren: Radiation characteristics of longitudinal waves from an antenna in a plasma, Radio Science **5**, 611 (1970).
[6] T. Ishizone, S. Adachi, Y. Mushiake and K. Sawaya: Experiments on electron plasma wave radiation and reception by some simple antennas, Summaries of Papers 1971 International Symp. of Antennas and Propagation, Sendai, Japan.
[7] F. L. Scarf, R. W. Fredricks, I. M. Green and C. T. Russel: Plasma waves in the day-side polar cusp 1. magnetospheric observations, J. Geophys. Res. **77**, 2274 (1972).
[8] T. Kawabe, Y. Kawai, O. Saka and Y. Nakamura: Glow mode plasma source for space chamber, Bulletin of the Institute of Space and Aeronautical Science, University of Tokyo **8**, 186 (1972). (in Japanese).
[9] H. H. Kuehl, G. E. Stewart and C. Yeh: Wave propagation in hot plasma waveguids with infinite magnetostatic fields, Phys. Fluids **8**, 723 (1965).
[10] Y. Kawai, Y. Nakamura, T. Itoh and T. Kawabe: Observation of free-streaming of electron in plasmas, IPPJ-145, Institute of Plasma Physics, Nagoya University, Nagoya, Japan.
[11] J. R. Apel: Nonlinear effects and turbulent behavior in a beam-plasma instability, Phys. Fluids **12**, 640 (1969).
[12] S. Prakash, B. H. Subbaraya and S. P. Gupta: Rocket measurements of ionization irregularities in the equatorial ionosphere at Thumba and identification of plasma instabilities, Indian J. Radio Space Phys. **1**, 72 (1972).
[13] T. Dote: Private communication.